JOURNAL OF COMPUTATIONAL PHYSICS 122, 291–299 (1995)

A Shock-Adaptive Godunov Scheme Based on the Generalised Lagrangian Formulation

C. Y. LEPAGE*

Department of Applied Mathematics, University of Waterloo, Waterloo, Ontario, Canada N2L 3G1

AND

W. H. HUI

Department of Mathematics, The Hong Kong University of Science & Technology, Clear Water Bay, Kowloon, Hong Kong

Received December 14, 1994

Application of the Godunov scheme to the Euler equations of gas dynamics based on the Eulerian formulation of flow smears discontinuities, sliplines especially, over several computational cells, while the accuracy in the smooth flow region is of the order $\mathcal{O}(h)$, where h is the cell width. Based on the generalised Lagrangian formulation (GLF) of Hui *et al.*, the Godunov scheme yields superior accuracy. By the use of coordinate streamlines in the GLF, the slipline—itself a streamline—is resolved crisply. Infinite shock resolution is achieved through the splitting of shock-cells. An improved entropy-conservation formulation of the governing equations is also proposed for computations in smooth flow regions. Finally, the use of the GLF substantially simplifies the programming logic resulting in a very robust, accurate, and efficient scheme.

1. INTRODUCTION

Recently, Hui and his collaborators [1–5] have introduced a generalised Lagrangian formulation (GLF) for the steady two-dimensional Euler equations of gas dynamics by mapping the Cartesian coordinates (x, y) to the Lagrangian-like coordinates (λ, ξ) by means of the transformation

$$dx = \frac{u}{q}\,d\lambda + U\,d\xi, \quad dy = \frac{v}{q}\,d\lambda + V\,d\xi, \tag{1}$$

where u and v are the x and y components of the velocity, $q = \sqrt{u^2 + v^2}$ is the speed of the flow, and U and V are geometric variables having dimensions of the reciprocal of the velocity. It can be observed from (1) that ξ defines a streamfunction while λ is the distance along a streamline. The transformed Euler equations in the GLF are

$$\frac{\partial \mathbf{E}}{\partial \lambda} + \frac{\partial \mathbf{F}}{\partial \xi} = 0, \tag{2}$$

where

$$\mathbf{E} = \begin{pmatrix} K \\ KH \\ Ku + pV \\ Kv - pU \\ U \\ V \end{pmatrix}, \quad \mathbf{F} = \begin{pmatrix} 0 \\ 0 \\ -p \sin\theta \\ p\cos\theta \\ -\cos\theta \\ -\sin\theta \end{pmatrix},$$

$$K = \rho(uV - vU),$$

$$H = \frac{1}{2}(u^2 + v^2) + \frac{\gamma}{\gamma - 1}\frac{p}{\rho},$$

$$\cos\theta = \frac{u}{q}, \quad \sin\theta = \frac{v}{q},$$

θ being the flow inclination angle, p the pressure, ρ the density, and γ the ratio of specific heats of the gas. The first four equations express the laws of conservation for mass, energy, and x and y momentum, in this order. The last two equations are the compatibility equations which arise from the transformation (1).

For supersonic flow, the system (2) is hyperbolic [5], and the classical Godunov scheme [6] for marching in the λ direction is applicable. The programming logic in the implementation of

* Now at Department of Mechanical Engineering, Concordia University, Montréal, Québec, Canada

0021-9991/95 $12.00

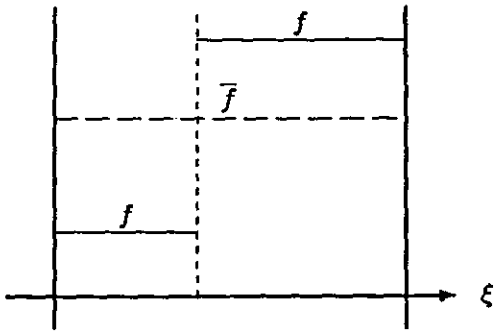

FIG. 1. Conserved average $\bar{f}$ across discontinuous data f.

the Riemann solver in the GLF is substantially simplified as a slipline, itself a streamline, coincides with a cell interface. This ensures the continuity of the fluxes across cell interfaces, i.e., coordinate streamlines, since the numerical flux vector $\mathbf{F}$ depends only on p and θ which are continuous across sliplines.

The ability of the Godunov scheme to resolve a slipline crisply is inherent to the GLF by the use of coordinate streamlines and has been formally demonstrated in [3]. In the favourable situation, a slipline coincides with a coordinate streamline and is resolved exactly; in other cases, the slipline is confined to lie within one computational cell and never cuts across other cells. The smearing effect induced by the averaging procedure across a slipline is thus avoided.

The intent of this paper is twofold: first, a treatment for the crisp resolution of shock discontinuities is proposed, with the methodology elaborated in Section 2; and second, an alternate entropy-conservation formulation is introduced in Section 3 for the Euler equations for purely smooth flow computations, with the added benefit of eliminating the small entropy overshoots commonly observed in the vicinity of sliplines. The complete numerical procedure is summarised in Section 4. Finally, several test problems are presented in Section 5 before closing with concluding remarks in Section 6.

2. THE SHOCK-ADAPTIVE GODUNOV SCHEME

The only source of error in the Godunov scheme arises from averaging the flow quantities over a computational cell when representing the flow in all cells by piecewise constant states. While this error is small in smooth flow regions, it is large in cells containing discontinuities. More precisely, the cell average

$$\bar{f} = \frac{1}{\Delta\xi}\int f\, d\xi$$

of a piecewise constant discontinuous distribution f, for example across a shock, is a poor representation, as shown in Fig. 1, of the two constant states on both sides of the discontinuity.

The basic idea of the shock treatment hereby proposed consists of splitting a *shock-cell*, a computational cell containing a shock wave, along the trajectory of the shock. The split shock-cell then consists of two *shock-subcells*: one entirely upstream of the shock and the other entirely downstream. In this way, the cell averaging procedure across the shock discontinuity is avoided. The fictitious cell boundary separating the two shock-subcells and moving through the underlying regular grid at the local speed of the shock shall be called a *partition*. With this abstraction, shock-subcells and regular cells can be treated on an equal footing in the Godunov scheme.

The elements of the method as applied to the Euler equations of gas dynamics based on the GLF are now outlined. This work is a generalisation of the shock-cell splitting method initiated in [4], where the shock position was assumed *a priori*, multiple shocks were excluded, and the shock speed was frozen within the shock-cell. More details on these recent developments can be found in [7].

Similar work, although based on the Eulerian formulation, has been reported in [8–11] among others. In addition to the necessity of a grid generation in the Eulerian formulation, for boundary value problems, the splitting of cells along shocks, and sliplines as well, constitutes quite a complex geometrical task. Such a method is commonly referred to as a *front-tracking* method in the literature as both shocks and sliplines are actively *tracked*. As already mentioned, as a consequence of using coordinate streamlines, sliplines need not be *tracked* in the GLF and shock-tracking becomes much simpler.

2.1. *Shock Propagation*

Figure 2 illustrates qualitatively the splitting of a shock-cell and the propagation of the shock through it. The subscripts d and u refer to the downstream and upstream flow states, respectively. The solution is marched in the usual sense, with the CFL stability condition being satisfied at all steps except at the last step when the shock leaves the shock-cell. This relaxation of the CFL condition is performed by ignoring incoming weak elementary waves in a shock-subcell in the deter-

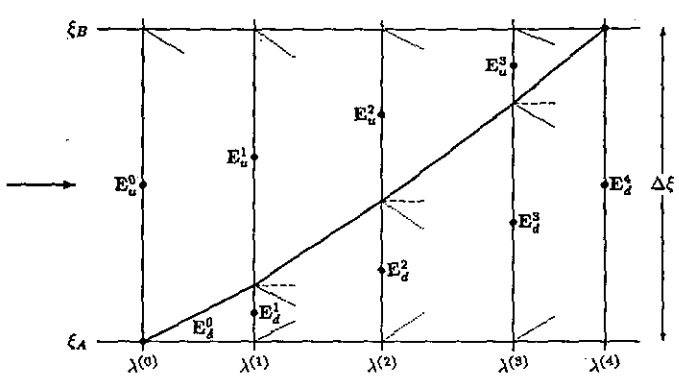

FIG. 2. Propagation of a shock through a shock-cell.

mination of the step size (see [8]). More precisely, an elementary wave is said to be *weak* if

$$\left|\frac{p_u}{p_d} - 1\right| < \text{Tol} \tag{3}$$

for some prescribed tolerance Tol. This procedure is exact for the case of an isolated shock propagating in a uniform flow region, but it leads to the loss of the conservative nature of the numerical scheme for a shock travelling in a non-uniform flow region. These effects, on the order of the tolerance Tol, are of no numerical significance. The numerical procedure for marching in λ is summarised in Section 4.

Regarding a shock-subcell as a normal cell with exactly one state, but with special interfaces, the cell-splitting concept extends straightforwardly to model complex shock interactions by recursively splitting a shock-subcell and introducing a new partition for every incoming shock. This intersection of two partitions, which models the collision of two shocks, is of special interest. Such a situation arises in the overtaking of shocks of the same family or in the intersection or reflection of shocks of different families. As is well known, a physical slipline will emanate from the intersection point of the two shocks. This new slipline can be captured exactly by introducing a new coordinate streamline at the intersection of the two partitions. However, adding a coordinate streamline has the disadvantage of possibly creating very small cells which in turn have the adverse effect of reducing the step size for the remainder of the simulation. It is generally preferable computationally to sacrifice the slipline resolution in order to avoid such refinement of the underlying grid and to have to take much smaller marching steps. This compromise is well justified since the slipline will be confined to lie within one cell in the GLF and no additional smearing will occur [3].

2.2. *Shock Detection Criterion*

The shock-adaptive Godunov scheme is complemented by a shock-cell splitting criterion which triggers the splitting of a shock-cell in the presence of a shock in the flow field. In the approach hereby considered, a shock-cell is split if the pressure jump across an elementary shock wave, as obtained from the exact solution to the local Riemann problem, is larger than some critical shock strength threshold, say if its reciprocal

$$\frac{p_u}{p_d} < \delta_{\text{SHK}}, \quad 0 < \delta_{\text{SHK}} < 1. \tag{4}$$

This desirable self-adaptivity feature permits for the automatic detection of a shock wave without *a priori* knowledge of its position nor existence.

The value of $\delta_{\text{SHK}} = 1$ corresponds to splitting all cells along elementary shock waves, whereas $\delta_{\text{SHK}} = 0$ corresponds to no splitting and the scheme simply reduces to the classical Godunov scheme. The choice $\delta_{\text{SHK}} = 1$ is obviously not a practical one since weak elementary shock waves, as identified by the solution to the local Riemann problems, are usually indicative of a compression region and not necessarily of a shock.

For a weak elementary shock wave, with $p_d/p_u = 1 + \varepsilon$, $0 < \varepsilon \ll 1$, the jump S_d/S_u in entropy measure $S = p/\rho^\gamma$ is $\mathcal{O}(\varepsilon^3)$. In terms of the criterion (4),

$$\frac{S_d}{S_u} \leq 1 + \frac{\gamma^2 - 1}{12\gamma^2}\left(\frac{1}{\delta_{\text{SHK}}} - 1\right)^3.$$

Thus, with a choice of $\delta_{\text{SHK}} = 0.70$ the entropy jump is less than 0.32%, and for shocks weaker than this the scheme degenerates to the classical Godunov scheme. Such a value of δ_{SHK} has been shown to be satisfactory for most computations.

The pressure ratio in (4) is cheaply computed since p_d and p_u are readily available from the solution to the local Riemann problems solved at all marching levels, and hence, minimal additional computational cost is incurred in the detection stage. The shock threshold δ_{SHK} is prescribed for a given problem.

2.3. *Implementation Considerations*

The principle of shock-cell splitting is conceptually easy, but the numerical implementation of the shock-adaptive scheme is not a straightforward task due to the irregularities in the computational domain caused by the moving shocks at each marching step. A double linked-list, schematically depicted in Fig. 3, is employed for the storage of the computational cells. This high-level object-oriented design is very advantageous in actively maintaining an irregular grid. This choice of list is motivated by the observation that every cell is bounded by two interfaces; and, in general, there is an interface between consecutive cells with the exception that at a solid boundary—a coordinate streamline—the list terminates with a cell interface.

The entry of an incoming shock in a cell is performed by inserting a new cell (the downstream shock-subcell) and a new interface (the partition) by updating the pointers $\leftrightarrow$ linking the new structures to the existing structures at the desired position in the list. The removal of a terminating shock-subcell is accomplished in a similar fashion, in which case the upstream shock-subcell, characterised by its zero width, is removed from the list along with its partition.

If in general a shock propagates through one cell to the next, this is not the case at a solid boundary where the shock is reflected and reenters the boundary cell. Other complications may also arise at the intersection of two shocks where the two shocks may be reflected or where one shock may overtake the other. In both cases, the common upstream shock-subcell is removed along with one of the partitions. The correct wave pattern is reestablished based on the solution to the local Riemann problem at the intersection point. The simplest approach

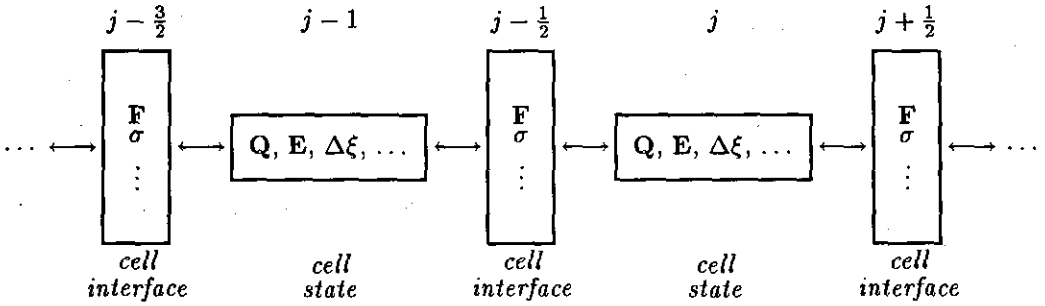

FIG. 3. Schematic representation of the linked-list used in the shock-adaptive scheme.

is thus to remove partition and cell pairs merging with cell interfaces even if this appears redundant when the shock simply propagates through the next cell. A new partition and cell pair will automatically be introduced at the next marching step to account for the incoming shock.

3. SMOOTH FLOW COMPUTATION

By the use of the shock-adaptive Godunov scheme based on the GLF, the error arising from averaging across discontinuities—shocks and sliplines—is prevented; hence, the numerical simulation of supersonic flow is effectively reduced to the computation of smooth flow. The utmost importance of the conservation form of the discretised equations (see Lax and Wendroff [12]) for the correct capturing of the flow discontinuities is no longer necessary since shocks and sliplines are now captured exactly, based on the information extracted from the Riemann problems. It is therefore possible to freely write the governing equations in non-conservation form and an entropy-conserving reformulation of the governing equations in the smooth flow region is proposed.

The motivation for the use of an alternate set of governing equations arises as a desire to eliminate the small entropy overshoots commonly observed in the vicinity of sliplines [3] despite the fact that the flow quantities are not averaged across a slipline in the GLF. This phenomenon is not unique to the GLF, but it is commonly observed when the Lagrangian formulation is used (see [13] as an example). A closer examination of the numerical solutions for various test problems indicates that the conserved variables are all monotonicity-preserving, except for the two geometrical variables U and V whose numerical errors contaminate the physical flow variables [7]. This suggests the replacement of the two compatibility equations by two equivalent equations.

Since the flow is isentropic along a streamline in a smooth flow region, one of the two compatibility equations in (2) is replaced by the law of conservation of entropy

$$\frac{\partial S}{\partial \lambda} = 0 \tag{5}$$

along a streamline. In contrast with the Eulerian formulation, the conservation of entropy equation provides an immediate first integral in the GLF. The conservation law of entropy (5) holds only in regions of smooth flow. Across a shock discontinuity, the exact entropy jump is imposed by the shock-adaptive scheme through the splitting of the shock-cell and the law of conservation of entropy (5) is applicable in the smooth flow regions upstream and downstream of the shock.

Along with the law of conservation of entropy, the conservation of mass and the conservation of energy equations provide three first integrals for S, H, and K along a streamline, hence this extension will be referred to as the SHK-formulation.

The proposed choice for the sixth independent governing equation of the SHK-formulation is

$$\frac{\partial \beta}{\partial \lambda} = -\frac{\sin(\theta+\beta)}{T}\frac{\partial \theta}{\partial \xi} \tag{6}$$

which is a combination of the two compatibility equations. In (6), $\beta = \tan^{-1}(U/V)$ defines the orientation angle of the distance line whereas $T = (U^2 + V^2)^{1/2}$ is a stretching factor defining the streamfunction. This choice of (6), which is not in conservative form, is mostly guided by numerical considerations, as the obtainment of β makes it possible to construct an entirely explicit decoding procedure (see Section 4). In contrast, a sixth equation for T, U, or V would give rise to a nonlinear equation to be solved iteratively, which is computationally costly. The resulting difference equation for (6) is

$$\beta_j^{n+1} = \beta_j^n - \frac{\Delta\lambda^n}{\Delta\xi_j}\frac{\sin(\theta_j^n+\beta_j^n)}{T_j^n}(\theta^*_{j+1/2} - \theta^*_{j-1/2}). \tag{7}$$

Equation (7) is not used in updating the flow state in a shock-subcell. The use of the strong conservative form of the governing equation (2) yields equivalently satisfactory results and has the advantage of being simpler to implement, given the trapezoidal geometry of a shock-subcell.

Finally, it should be emphasised that all primary physical flow variables are conserved; that is, the mass, the energy, the entropy, and the x and y components of the momentum are

conserved—only the geometrical variable β is not. Moreover, in the GLF, the conservation laws of mass, energy, and entropy are satisfied analytically and only that of momentum are satisfied numerically. By contrast, all the physical conservation laws are satisfied numerically in the Eulerian formulation.

4. NUMERICAL IMPLEMENTATION

The computational procedure for the shock-adaptive Godunov scheme is summarised in the following seven steps:

Step 1. *Initiation at* λ^0. Given a flow problem in the physical xy-plane, an initial distance line Γ, not itself a streamline, is chosen where the flow is known (e.g., a given uniform flow) and identified as the distance line $\lambda = 0$ in the computational $\lambda\xi$-plane. The curve Γ is parametrised by the streamfunction ξ for $\xi_0, \xi_1, \ldots, \xi_N$. In most cases, the initial distance line Γ can be chosen to be orthogonal to the given uniform flow and ξ can be taken as the arclength of Γ. This results in $T_j^0 = 1$ and $\beta_j^0 = -\theta_j^0$. $\mathbf{E}_j^0$ is then known at $\lambda = 0$ for all j by taking the average within the cells. Further, no assumption is made regarding the presence of shocks as they will be automatically detected.

Step 2. *Solution of the local Riemann problems, at* λ^n, *for all adjacent cell pairs.* With the flow states $\mathbf{Q}_j^n = (p, \rho, M, \theta)_j^n$ known for all cells at distance step n, a local Riemann problem is solved at all cell interfaces, including partitions, for all adjacent cell pairs. The flow states are assumed constant within all cells. A Newton iterative method is employed (see [7, 14]) for solving the exact Riemann problems for p^* and θ^* immediately downstream of the elementary $\pm$ waves. At a partition, the initial guess for the downstream pressure p^*, in the Newton iterative procedure, is taken as the pressure value in the downstream shock-subcell to expedite the convergence. The numerical fluxes

$$(\mathscr{F}^{\pm})_j^n = \begin{cases} \mathbf{F}(p_j^n, \theta_j^n) & \text{if } \pm\sigma_{j\pm1/2}^n < 0 \\ \mathbf{F}(p_{j\pm1/2}^*, \theta_{j\pm1/2}^*) + \sigma_{j\pm1/2}^n (\mathbf{E}_j^n - \mathbf{E}_{j\pm1/2}^*) & \text{if } \pm\sigma_{j\pm1/2}^n \geq 0, \end{cases} \tag{8}$$

are evaluated at $\xi_{j\pm1/2}$ where $\sigma_{j\pm1/2}^n$ are the slopes $d\xi/d\lambda$ of the interface $\xi_{j\pm1/2}$ at λ^n and $\mathbf{E}_{j\pm1/2}^*$ is the averaged conserved flow state along the inner (downstream) side of the shock relative to the shock-subcell being updated. It is easy to see that the composite flux is multi-valued at a partition $\xi_{j+1/2}$ since $(\mathscr{F}^+)_j^n \neq (\mathscr{F}^-)_{j+1}^n$. The speeds $\sigma_{j\pm1/2}^n$ of the partitions are updated based on the speeds of the corresponding elementary shock waves in the local Riemann problems.

The presence of a new shock is tested at all cell interfaces. If the cell splitting criterion (4) is satisfied, a new partition is introduced to account for the incoming shock and the cell is split.

At a boundary cell, the flow tangency angle θ_b^n is computed for the given problem and the boundary Riemann problem with initial data $(p, \rho, M, \theta)_j^n$ and $(p, \rho, M, 2\theta_b - \theta)_j^n$ is solved. This procedure effectively treats the boundary as a slipline with local inclination angle θ_b^n.

Step 3. *Determination of the step size* $\Delta\lambda^n$. To satisfy the stability condition of the scheme, the step size is determined as the minimum of the step sizes

$$\Delta\lambda^n = \nu \Big/ \max_j \left\{ \frac{|\sigma_{j\pm1/2}^n|}{\Delta\xi_j} \right\} \tag{9}$$

for the regular cells and

$$\Delta\lambda^n = \min_j \left\{ \frac{\Delta\xi_j}{(|\sigma_{j+1/2}^n| + |\sigma_{j-1/2}^n|)} \right\}, \tag{10}$$

for the shock-subcells which represents the intersection point of the $\pm$ waves in the shock-subcell, or equivalently, the intersection point of the incoming elementary wave with the opposing cell interface, also an elementary wave. The prescribed CFL number ν is taken to be constant throughout the computations.

For an elementary Prandtl–Meyer expansion, $\sigma_{j\pm1/2}^n$ is replaced by the speed of the leading Mach line (fastest characteristic). For an elementary shock wave, $\sigma_{j\pm1/2}^n$ is replaced by the shock speed, since any disturbance propagating in the shock direction is bounded by the shock with the flow upstream of the shock being undisturbed.

It should, however, be observed that under the strict application of (10), a shock cannot formally leave a shock-cell due to the recursive refinement of the step size in the upstream shock-subcell. To avoid such a constraint, the CFL condition is relaxed according to (3) and the step size is adjusted such that the shock leaves the shock-cell exactly at a coordinate streamline. The shock is then re-introduced at the next marching level on the basis of the solution to the local Riemann problem at that streamline.

Step 4. *Advancement of the average cell states from* λ^n *to* $\lambda^{n+1} = \lambda^n + \Delta\lambda^n$. The average states $\mathbf{E}_j^{n+1}$ for all non-terminating cells, with domain

$$\{(\lambda, \xi) \in \mathbb{R}^2 \,\|\, \lambda^n < \lambda < \lambda^{n+1},\ \xi_{j-1/2}^n + \sigma_{j-1/2}^n(\lambda - \lambda^n) < \xi < \xi_{j+1/2}^n + \sigma_{j+1/2}^n(\lambda - \lambda^n)\},$$

are obtained at λ^{n+1} using the difference equation

$$\mathbf{E}_j^{n+1} = \mathbf{E}_j^n - \frac{\Delta\lambda^n}{\Delta\xi_j^{n+1}} ((\mathscr{F}^+)_j^n - (\mathscr{F}^-)_j^n) \tag{11}$$

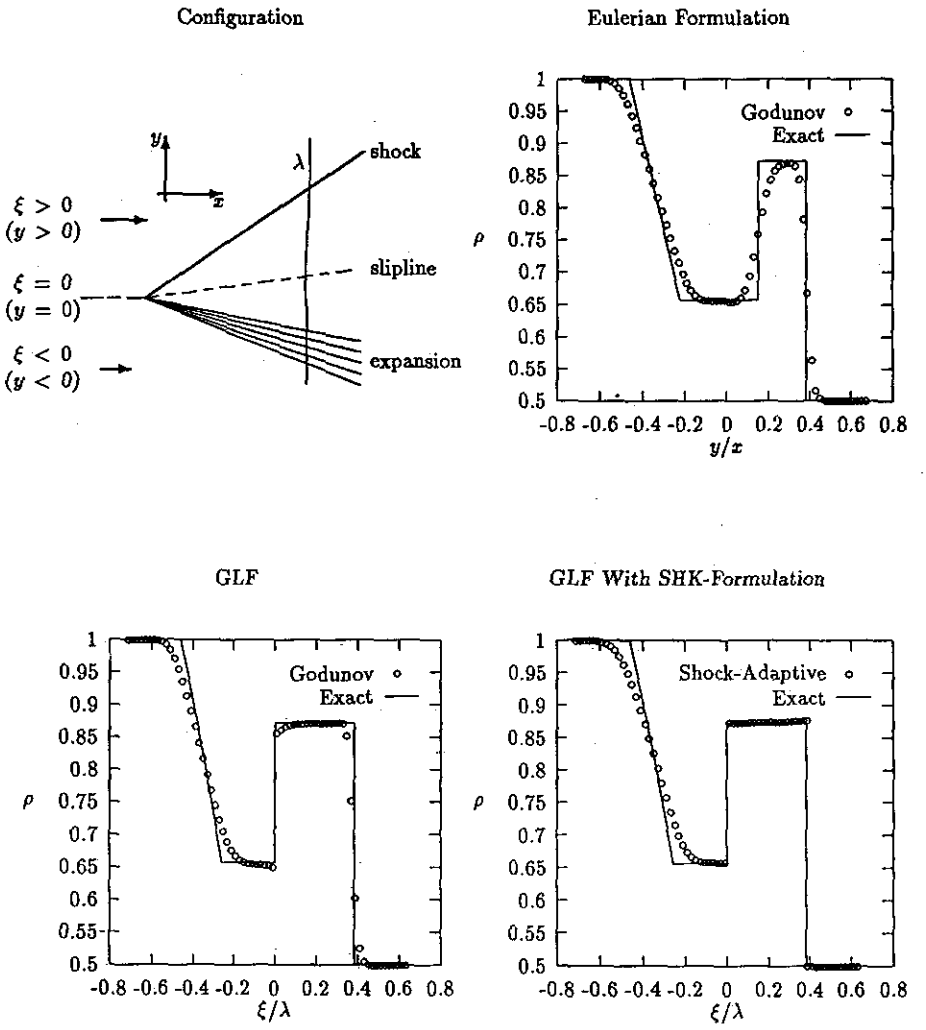

FIG. 4. Density profiles of the numerical solution to a Riemann problem.

with the composite fluxes given by (8).

The cell width $\Delta\xi_j^{n+1}$ of a shock-subcell is updated using

$$\Delta\xi_j^{n+1} = \Delta\xi_j^n + (\sigma_{j+1/2}^n - \sigma_{j-1/2}^n)\,\Delta\lambda^n \tag{12}$$

prior to advancing the conserved flow state. For a fixed coordinate streamline, $\sigma_{j+1/2}^n = 0$; for a partition, $\sigma_{j+1/2}^n = \sigma_{\text{shock}}^n$, as obtained from the solution to the local Riemann problem.

For a regular rectangular cell, the above difference equation reduces to the familiar updating formula used in the classical Godunov scheme.

Step 5. *Obtainment of the flow variables* $\mathbf{Q}_j^{n+1} = (p, \rho, M, \theta)_j^{n+1}$ *at* λ^{n+1}. The average states $\mathbf{E}_j^{n+1}$, denoted here by $(e_1, e_2, e_3, e_4, e_5, e_6)^T$ for convenience, are decoded in order to obtain the new values of the physical flow variables at λ^{n+1}. For the flow quantities (H, K, e_3, e_4, β) known at λ^{n+1}, with β given either by (7) or by $\beta = \tan^{-1}(e_5/e_6)$, let

$$A = -\frac{\gamma+1}{\gamma-1},$$

$$B = \frac{1}{\gamma-1}(e_3\cos\beta - e_4\sin\beta),$$

$$C = (e_3)^2 + (e_4)^2 - 2K^2H;$$

then the product pT satisfies the quadratic equation

$$A(pT)^2 + 2B(pT) + C = 0$$

with discriminant $\Delta = B^2 - AC \geq 0$ for supersonic flow.

For the usage of the governing equations (2) in conservative form, with e_5 and e_6 known,

$$T = \sqrt{(e_5)^2 + (e_6)^2}$$

and the appropriate solution for the pressure is

$$p = \frac{-B + \sqrt{\Delta}}{TA}.$$

Or, in the case of the SHK-formulation, with S known,

$$p = \left[\left(\frac{\gamma - 1}{2}\right)\frac{(-B + \sqrt{\Delta})^2 - A^2C}{A^2K^2S^{1/\gamma}}\right]^{\gamma/(\gamma-1)}$$

with corresponding T value

$$T = \frac{-B + \sqrt{\Delta}}{pA}.$$

Note that, for the SHK-formulation, β_j^{n+1} is directly obtained from (7) and the U and V equations need not be updated.

Finally, the other flow variables are obtained using

$$u = \frac{e_3 - pT\cos\beta}{K},$$

$$v = \frac{e_4 + pT\sin\beta}{K},$$

$$\rho = \frac{K}{T(u\cos\beta - v\sin\beta)}.$$

M and θ are obtained from their definitions.

Step 6. Elimination of the terminating shock-subcells, at λ^{n+1}. The shock-subcells terminating at λ^{n+1} are eliminated by removing the corresponding partitions and the upstream shock-subcells. This renders the downstream subcell a regular cell at λ^{n+1}.

Step 7. Repeat steps 2–7 to march forward in λ.

5. NUMERICAL EXPERIMENTS

Flows dominated by shock waves are simulated to illustrate the advantages of the shock-adaptive scheme. A CFL number

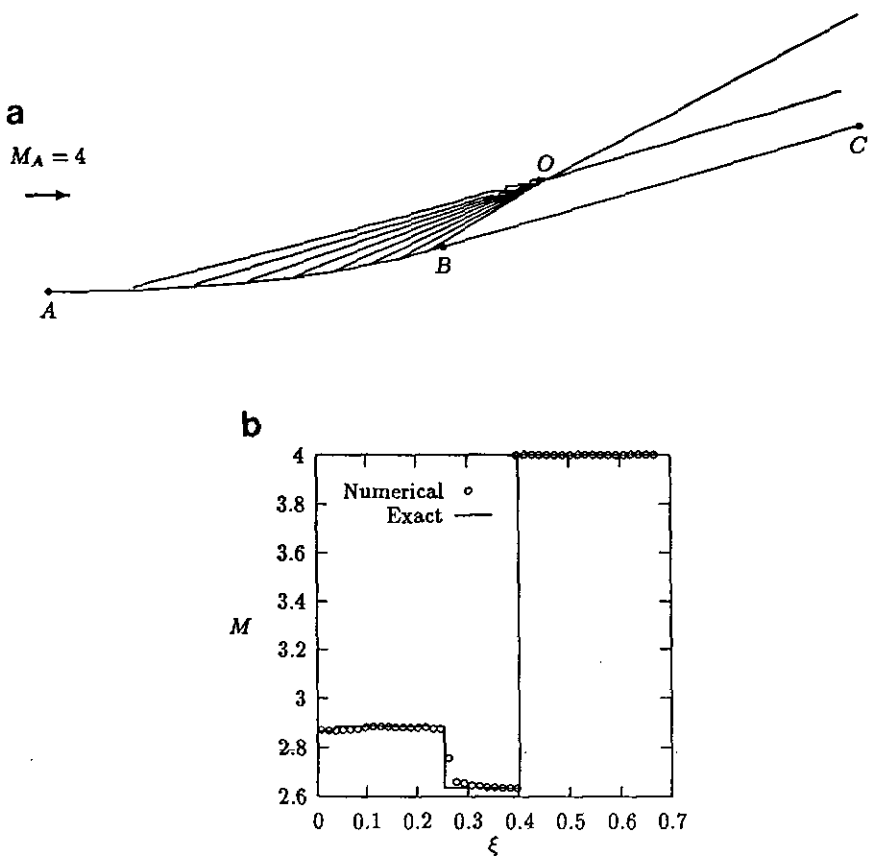

FIG. 5. Sudden formation of a shock wave: (a) computed Mach contours; (b) computed mach profile along a distance line downstream of O.

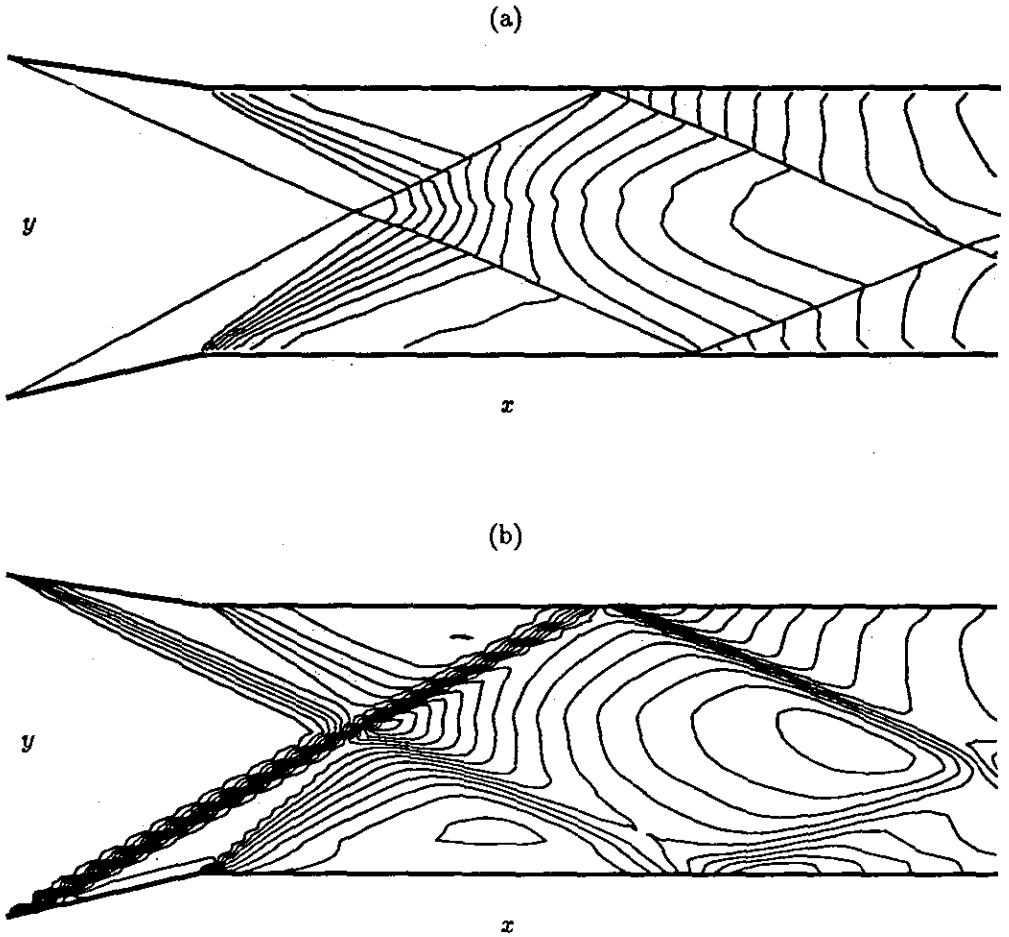

FIG. 6. Temperature contours in a supersonic channel using: (a) the shock-adaptive scheme based on the GLF, with SHK-formulation; (b) the classical Godunov scheme based on the GLF.

of 0.90 is used in all computations; the shock threshold is $\delta_{SHK} = 0.70$, except for the second example for which it is 0.90.

The first example consists of the constant-state two-dimensional Riemann problem with initial parallel flow data,

$$(p, \rho, M, \theta) = \begin{cases} (0.25, 0.5, 4.0, 0.0) & \text{if } \xi > 0, \\ (1.0, 1.0, 2.4, 0.0) & \text{if } \xi < 0. \end{cases}$$

The computed density profiles of the numerical solution are plotted in Fig. 4 to show the evolution of the shock-adaptive scheme at various stages in its development. For the Godunov scheme based on the Eulerian formulation, both shock and slipline are smeared over several computational cells, the slipline resolution being much poorer. By use of the GLF, the Godunov scheme can resolve the slipline very crisply while there is a small improvement in the shock resolution, the latter improvement being due to the compressive nature of the GLF. Finally, the shock-adaptive scheme resolves the shock to infinite order. At the slipline, the pressure is continuous and by correcting the numerical entropy by the use of the SHK-formulation, the overshoots in density observed near the slipline have been consequently eliminated.

The second example, suggested by Johannesen in [15] and whose exact solution is given by Hui and Zhao in [3], consists of a uniform free stream supersonic flow $M_\infty = 4.0$ past a specially designed airfoil such that a shock of finite strength is formed suddenly in the interior of the flow field, with the creation of a slipline and a Prandtl–Meyer expansion wave at the point O of origin of the shock (see Fig. 5(a)). This benchmark problem is computationally challenging due to the concentration of all characteristics at the point O. A hypersensitive shock threshold of $\delta_{SHK} = 0.90$ (with entropy jump less than 0.0056%) is used to correctly capture the shock at its earliest stage in formation. The method is complemented by a second-order scheme which accounts for the curvature of the airfoil [7]. The results are shown in Fig. 5, where it can be seen that the flow discontinuities are captured crisply. Although the expansion wave is not visible in the contour plot, it is slightly perceptible in the Mach number profile plot.

In the last example, the steady flow in a two-dimensional supersonic channel with wedge angles of 15° and −10° is considered. The uniform upstream flow Mach number is $M_\infty = 3.0$. The computations use 25 uniform cells across the channel. The normalised temperature contours for the shock-adaptive Godunov scheme are plotted in Fig. 6 and compared to the solution obtained by the classical Godunov scheme. The manifest sharpness of the temperature contours in Fig. 6(a) clearly demonstrates the superiority of the shock-adaptive scheme over the classical Godunov scheme. Further, the slipline emanating from the intersection point of the two incident shocks is perceptible using the shock-adaptive scheme, but totally blurred using the classical Godunov scheme.

It should be noted that the average number of iterations required to solve an exact Riemann problem to within a tolerance of 10^{-6} is lower for the shock-adaptive scheme than for the classical Godunov scheme, to 1.57 from 1.71 in the first example and to 2.04 from 2.24 in the third example (and increasingly lower if the method is used in conjunction with a second-order scheme [7]). The explanation is simple: with the shocks being detected, it is possible to use a very accurate initial guess in the iterative procedure. However, the extra marching steps required in the shock-adaptive scheme due to the additional restriction (10) to the CFL condition for shock-subcells outweigh the reduction in the average number of iterations per Riemann problem solved. Nonetheless, despite its higher cost, the shock-adaptive scheme is much more cost-efficient than the classical Godunov scheme as much greater accuracy is achieved, as witnessed in the numerical examples.

6. CONCLUSIONS

While comparable resolution of flow discontinuities—shocks and sliplines—can be and has been achieved using front-tracking methods based on the Eulerian formulation [11], the present methodology based on the generalised Lagrangian formulation ensures the exact conservation of mass, energy, and entropy; solves boundary value problems without the need to generate a computational grid; and crisply resolves sliplines by use of coordinate streamlines and shocks by use of an adaptive shock-cell splitting technique. Furthermore, the programming logic required in the computer implementation is substantially simpler in comparison with the Eulerian formulation: first, the wave structure of the Riemann solution in the GLF is much simpler in relation to the coordinate system; second, unlike the Eulerian formulation which necessitates the tracking of both shocks and sliplines, only shocks need to be tracked in the GLF; and finally, the computational domain for boundary value problems is always regular. All these advantages result in a highly efficient, accurate, and robust numerical scheme.

ACKNOWLEDGMENTS

This research was sponsored by NSERC of Canada, NASA of U.S., and RGC of Hong Kong.

REFERENCES

1. W. H. Hui and H. J. Van Roessel, AGARD CP-386, 1985 (unpublished).
2. C. Y. Loh and W. H. Hui, *J. Comput. Phys.* **89,** 207 (1990).
3. W. H. Hui and C. Y. Loh, *J. Comput. Phys.* **103,** 450 (1992).
4. W. H. Hui and C. Y. Loh, *J. Comput. Phys.* **103,** 465 (1992).
5. W. H. Hui and Y. C. Zhao, *Proceedings, Fourth International Conference on Hyperbolic Problems*, edited by A. Donato and F. Oliveri, Notes on Numerical Fluid Mechanics, (Vieweg & John, Wiesbaden, 1993).
6. S. K. Godunov, *Mat. Sb.* **47,** 271 (1959).
7. C. Lepage, Master of Mathematics thesis, University of Waterloo, 1993 (unpublished).
8. B. K. Swartz and B. Wendroff, *Appl. Numer. Math.* **2,** 385 (1986).
9. A. Harten and J. M. Hyman, *J. Comput. Phys.* **50,** 235 (1983).
10. N. H. Risebro and A. Tveiko, *SIAM J. Sci. Stat. Comput.* **55,** 1401 (1991).
11. R. J. Leveque and K. M. Shyue, Technical Report No. 92-3, University of Washington, 1992 (unpublished).
12. P. D. Lax and B. Wendroff, *Comm. Pure Appl. Math.* **13,** 217 (1960).
13. M. Ben-Artzi and J. Falcovitz, *J. Comput. Phys.* **55,** 1 (1984).
14. T. G. Sheidow, Master of Mathematics thesis, University of Waterloo, 1991 (unpublished).
15. N. H. Johannesen, *Philos. Mag.* **43,** 568 (1952).